coding region can theoretically form a stable RNA secondary structure with the *rtpA* start codon region. This predicted paired structure would be expected to inhibit translation initiation at the *rtpA* start codon. Substitution of the three Trp codons of *rtpLP* by Ala codons would reduce the stability of this RNA secondary structure, thereby preventing RNA secondary structure inhibition of AT synthesis. Complicating this simple interpretation is the prediction that the *rtpLP* coding region can also pair with the sequence just upstream of the *rtpLP* start codon. Thus, competitive RNA-RNA interactions may contribute to the extent of inhibition of *rtpA* translation.

Despite these complications, our studies show that both transcriptional and translational sensing of uncharged $tRNA^{Trp}$ are used by *B. subtilis* to regulate *trp* operon expression. *Escherichia coli* also senses uncharged $tRNA^{Trp}$ translationally in regulating *trp* operon expression; however, the mechanism of action is very different (*19*).

References and Notes

1. D. Henner, C. Yanofsky, in Bacillus subtilis *and Other Gram-Positive Bacteria: Biochemistry, Physiology and Molecular Genetics,* A. L. Sonenshein, J. A. Hoch, R. Losick, Eds. (American Society for Microbiology, Washington, DC, 1993), pp. 269–280.
2. P. Gollnick, P. Babitzke, E. Merino, C. Yanofsky, in Bacillus subtilis *and Its Closest Relatives: From Genes to Cells,* A. L. Sonenshein, J. A. Hoch, R. Losick, Eds. (American Society for Microbiology, Washington, DC, 2001), pp. 233–244.
3. P. Babitzke, P. Gollnick, *J. Bacteriol*. **183**, 5795 (2001).
4. P. Babitzke, J. T. Stults, S. J. Shire, C. Yanofsky, *J. Biol. Chem*. **269**, 16597 (1994).
5. A. A. Antson *et al*., *Nature* **374**, 693 (1995).
6. A. A. Antson *et al*., *Nature* **401**, 235 (1999).
7. P. Babitzke, C. Yanofsky, *Proc. Natl. Acad. Sci. U.S.A.* **90**, 133 (1993).
8. J. Otridge, P. Gollnick, *Proc. Natl. Acad. Sci. U.S.A.* **90**, 128 (1993).
9. P. Babitzke, D. G. Bear, C. Yanofsky, *Proc. Natl. Acad. Sci. U.S.A.* **92**, 7916 (1995).
10. H. Shimotsu, M. I. Kuroda, C. Yanofsky, D. J. Henner, *J. Bacteriol*. **166**, 461 (1986).
11. M. Yang, A. de Saizieu, A. P. Loon, P. Gollnick, *J. Bacteriol*. **177**, 4272 (1995).
12. H. Du, R. Tarpey, P. Babitzke, *J. Bacteriol*. **179**, 2582 (1997).
13. H. Du, P. Babitzke, *J. Biol. Chem*. **273**, 20494 (1998).
14. E. Merino, P. Babitzke, C. Yanofsky, *J. Bacteriol*. **177**, 6362 (1995).
15. W. Steinberg, *J. Bacteriol*. **117**, 1023 (1974).
16. A. I. Lee, J. P. Sarsero, C. Yanofsky, *J. Bacteriol*. **178**, 6518 (1996).
17. J. P. Sarsero, E. Merino, C. Yanofsky, *Proc. Natl. Acad. Sci. U.S.A.* **97**, 2656 (2000).
18. T. M. Henkin, *Curr. Opin. Microbiol*. **3**, 149 (2000).
19. A. Valbuzzi, C. Yanofsky, *Science* **293**, 2057 (2001).
20. Cultures to be examined for AT levels were grown under the conditions described in the figure legends. The cell pellet from 1 ml of each culture (at the same density) was suspended in 20 μl of SDS–tris-Tricine sample buffer and placed in a boiling-water bath for 5 min. Samples were centrifuged and the supernatants were transferred to fresh tubes; 5 μl of each sample was electrophoresed on an SDS–15% polyacrylamide gel in tris-Tricine buffer systems (*21*) and then electrophoretically transferred to a pure nitrocellulose transfer-immobilization membrane (Protran BA79; Schleicher & Schuell Inc.). Immunoblotting was performed as described (*22*) with rabbit polyclonal antisera to the AT protein. Bound antibody was visualized with horseradish peroxidase–conjugated donkey antibody to rabbit immunoglobulin (Amersham) and SuperSignal West Pico Chemiluminescent detection reagents (Pierce). The Western blot bands were quantified with the Molecular Analyst 2.1 software package.
21. H. Schagger, G. von Jagow, *Anal. Biochem*. **166**, 368 (1987).
22. W. N. Burnett, *Anal. Biochem*. **112**, 195 (1981).
23. S. Shudershana, H. Du, M. Mahalanabis, P. Babitzke, *J. Bacteriol*. **181**, 5742 (1999).
24. J. Sekiguchi, N. Takada, H. Okada, *J. Bacteriol*. **121**, 688 (1975).
25. H. J. Vogel, D. M. Bonner, *J. Biol. Chem*. **218**, 97 (1956).
26. T. E. Creighton, C. Yanofsky, *Methods Enzymol*. **17**, 365 (1969).

27. We thank A. Valbuzzi, F. Gong, and J. Sarsero for stimulating discussions and valuable technical advice and C. Squires, F. Gong, P. Babitzke, P. Gollnick, and A. Valbuzzi for critical reading of the manuscript. Supported by NSF grant MCB-0093023.

25 March 2003; accepted 9 June 2003

A B Cell–Based Sensor for Rapid Identification of Pathogens

Todd H. Rider,[1]* Martha S. Petrovick,[1] Frances E. Nargi,[1] James D. Harper,[1] Eric D. Schwoebel,[1] Richard H. Mathews,[1] David J. Blanchard,[1] Laura T. Bortolin,[1] Albert M. Young,[1] Jianzhu Chen,[2] Mark A. Hollis[1]

We report the use of genetically engineered cells in a pathogen identification sensor. This sensor uses B lymphocytes that have been engineered to emit light within seconds of exposure to specific bacteria and viruses. We demonstrated rapid screening of relevant samples and identification of a variety of pathogens at very low levels. Because of its speed, sensitivity, and specificity, this pathogen identification technology could prove useful for medical diagnostics, biowarfare defense, food- and water-quality monitoring, and other applications.

The diagnosis of infectious diseases such as severe acute respiratory syndrome (SARS) and detection of potential bioterrorism agents such as *Bacillus anthracis* (anthrax) and variola major (smallpox) would benefit greatly from a pathogen identification method with better combined speed and sensitivity than existing methods such as immunoassays (*1*) and polymerase chain reaction (PCR) (*2*). This report describes a pathogen sensor that achieves an optimal combination of speed and sensitivity through the use of B lymphocytes: members of the adaptive immune system that have evolved to identify pathogens very efficiently. B cell lines were engineered to express cytosolic aequorin, a calcium-sensitive bioluminescent protein from the *Aequoria victoria* jellyfish (*3*, *4*), as well as membrane-bound antibodies specific for pathogens of interest. Cross-linking of the antibodies by even low levels of the appropriate pathogen elevated intracellular calcium concentrations within seconds (*5*), causing the aequorin to emit light (*6*, *7*). We named the sensor CANARY (cellular analysis and notification of antigen risks and yields).

We first developed a system for efficient production of pathogen-specific B cell lines. A parental cell line with stable expression of cytosolic aequorin (*8*) was generated from the M12g3R (IgM+) B cell line (*9*), and the clone with maximum light emission upon cross-linking of the surface immunoglobulin M (IgM) was selected (*10*). The M12g3R-aequorin cells were subsequently transfected with plasmids containing antibody light- and heavy-chain constant-region genes, into which variable regions specific for a particular pathogen were inserted. Clones from the second transfection were selected for optimal response to that pathogen (*10*).

The resulting cells responded to pathogens with excellent speed, sensitivity, and specificity. Cells specific for *Yersinia pestis*, the bacterium that causes plague, could detect as few as 50 colony-forming units (CFU) in a total assay time of less than 3 min, which included a concentration step (Fig. 1A). The probability of detection for *Y. pestis* ranged from 62% for 20 CFU to 99% for 200 CFU (fig. S1), whereas the false-positive rate for the CANARY assay was 0.4%. These cells did not respond to large numbers of unrelated bacteria (*Francisella tularensis*), nor did excess *F. tularensis* block the response to very low levels of *Y. pestis*. Similar performance was observed with other cell lines, including one specific for orthopoxviruses (Fig. 1B). The sensitivity of a B cell line specific for Venezuelan equine encephalitis (VEE) virus, a virus too small to be concentrated in a microcentrifuge (*10*), is currently 5×10^5 plaque-forming units (PFU) (Fig. 1C).

CANARY can also identify pathogens in complex relevant samples. B cells specific for *Escherichia coli* strain O157:H7, an im-

[1]Massachusetts Institute of Technology Lincoln Laboratory, Lexington, MA 02420, USA. [2]Center for Cancer Research and Department of Biology, Massachusetts Institute of Technology, Cambridge, MA 02139, USA.

*To whom correspondence should be addressed. E-mail: thor@ll.mit.edu

portant pathogen found in vegetable, fruit, and meat products (*11*), detected as little as 500 CFU/g in lettuce in less than 5 min, which included the initial sample preparation time (Fig. 2A). These results compare favorably with reports describing the detection of bacteria in food with PCR protocols that take 30 to 60 min and achieve a limit of detection of 10 to 10,000 CFU per gram or per milliliter (*12*, *13*). Rapid pathogen identification methods are necessary to ensure timely accurate diagnosis of disease in patients with infections requiring immediate treatment (*14*). CANARY can detect as few as 1000 CFU of *B. anthracis* spores extracted from seeded nasal swabs (Fig. 2B), demonstrating the potential to rapidly screen patients for inhalation anthrax exposure.

The cell preparation protocol that yields optimal performance requires less than 1 hour of labor over 2 days (*10*) and can be performed on a scale that cost-effectively prepares enough cells for millions of assays. Prepared cells can be stored at room temperature for at least 2 days; refrigerated for at least 2 weeks; or frozen indefinitely, while retaining full activity.

The pathogen sensor described here provides an optimal combination of speed and sensitivity that is currently unmatched by any other identifier. Currently available immunoassay methods require at least 15 min and have a much higher limit of detection (*1*). Although an ultrafast PCR with detection of 5 CFU in only 9 min has been reported (*2*), the total assay requires at least 20 to 30 min to complete when coupled with the fastest sample-preparation technology (*15*). Another feature of CANARY is that the antibody expressed determines the cell specificity and can be tailored to a desired application. We have produced B cell lines that respond to just a single strain of foot-and-mouth disease virus (fig. S2) or to many strains of VEE virus (fig. S3), as well as cells that

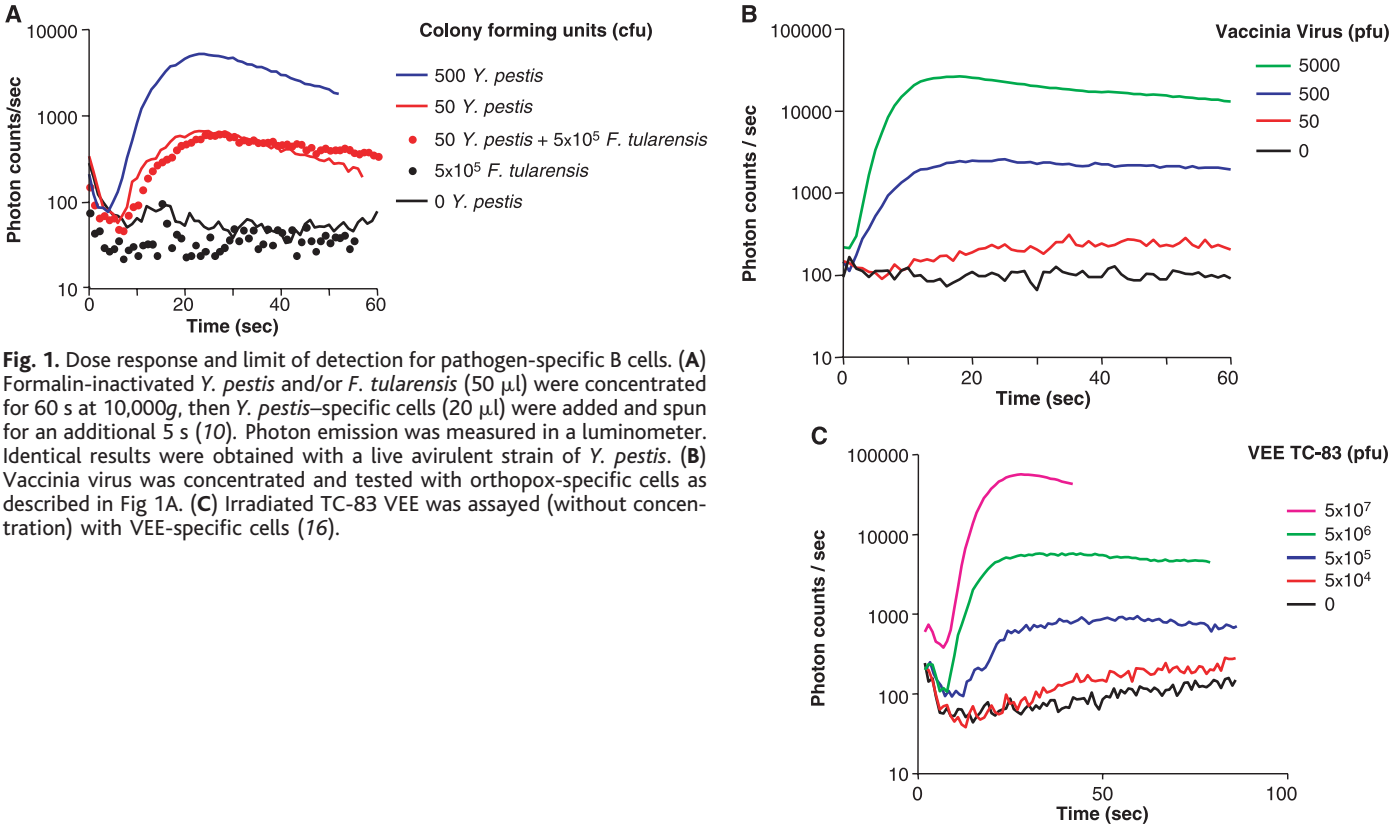

Fig. 1. Dose response and limit of detection for pathogen-specific B cells. (**A**) Formalin-inactivated *Y. pestis* and/or *F. tularensis* (50 μl) were concentrated for 60 s at 10,000*g*, then *Y. pestis*–specific cells (20 μl) were added and spun for an additional 5 s (*10*). Photon emission was measured in a luminometer. Identical results were obtained with a live avirulent strain of *Y. pestis*. (**B**) Vaccinia virus was concentrated and tested with orthopox-specific cells as described in Fig 1A. (**C**) Irradiated TC-83 VEE was assayed (without concentration) with VEE-specific cells (*16*).

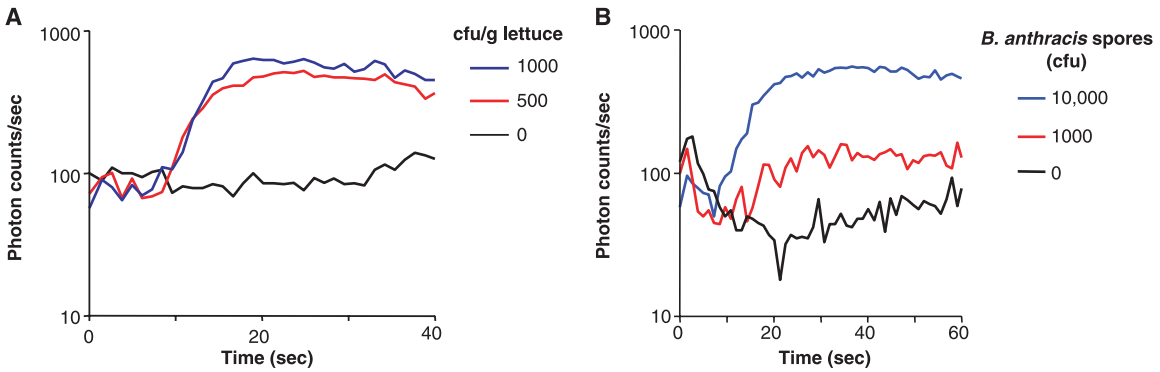

Fig. 2. Detection of pathogens in samples. (**A**) Lettuce (25 g) was contaminated with the indicated amounts of inactivated *E. coli* O157:H7 and shaken in sterile bags with extraction medium (assay medium without fetal bovine serum). The supernatant was passed through a 5-μm filter to remove large particulates, the eluate was centrifuged, and the liquid was replaced with assay medium. The samples were tested as described in Fig. 1 with cells that respond to *E. coli* O157:H7. (**B**) Nasal passages were wiped with sterile cotton swabs, which were subsequently seeded with 10,000 or 1000 CFU of formalin-inactivated *B. anthracis* Sterne-strain spores. Nasal swabs were extracted in 1 ml of extraction medium, and the samples were treated as described for the lettuce supernatant in (A). The treated samples were tested as described in Fig. 1 with a B cell line engineered to respond to *B. anthracis* spores.

distinguish pathogenic O157:H7 *E. coli* from nonpathogenic *E. coli* strains (fig. S4). The speed, sensitivity, and specificity of CANARY are valuable attributes for applications including medical and agricultural diagnostics, biowarfare defense, and food- and water-quality monitoring.

References and Notes

1. C. A. Rowe *et al.*, *Anal. Chem.* **71**, 3846 (1999).
2. P. Belgrader *et al.*, *Science* **284**, 449 (1999).
3. M. J. Cormier, D. C. Prasher, M. Longiaru, R. O. McCann, *Photochem. Photobiol.* **49**, 509 (1989).
4. O. Shimomura, B. Musicki, Y. Kishi, *Biochem. J.* **261**, 913 (1989).
5. H. A. Wilson *et al.*, *J. Exp. Med.* **166**, 601 (1987).
6. F. I. Tsuji *et al.*, *Proc. Natl. Acad. Sci. U.S.A.* **83**, 8107 (1986).
7. O. Shimomura, F. H. Johnson, *Proc. Natl. Acad. Sci. U.S.A.* **75**, 2611 (1978).
8. D. Button, M. Brownstein, *Cell Calcium* **14**, 663 (1993).
9. V. S. Parikh *et al.*, *J. Exp. Med.* **174**, 1103 (1991).
10. Materials and methods are available as supporting material on *Science* Online.
11. M. L. Ackers *et al.*, *J. Infect. Dis.* **177**, 1588 (1998).
12. R. Lindqvist, *Int. J. Food Microbiol.* **37**, 73 (1997).
13. A. J. Hough, S. A. Harbison, M. G. Savill, L. D. Melton, G. Fletcher, *J. Food Prot.* **65**, 1329 (2002).
14. L. A. Lucore, M. A. Cullison, L. A. Jaykus, *Appl. Environ. Microbiol.* **66**, 1769 (2000).
15. F. Pourahmadi *et al.*, *Clin. Chem.* **46**, 1151 (2000).
16. J. T. Roehrig, J. H. Mathews, *Virology* **142**, 347 (1985).

17. We appreciate the following generous donations: M12g3R B cell line, P. Tucker (University of Texas, Austin); pCMV.AEQ.IRES.NEO plasmid, D. Button (Stanford University); VKExpress, Invitrogen Corporation; *B. anthracis* Sterne, antibody to orthopoxvirus, and TC-83 VEE, G. Ludwig (U.S. Army Medical Research Institute of Infectious Diseases); antibody to *Y. pestis* sequence and inactivated bacteria, Naval Medical Research Center; antibody to *B. anthracis* spore, J. Kearney (University of Alabama, Birmingham); and antibody to VEE and inactivated VEE, J. Roehrig (Centers for Disease Control and Prevention, Fort Collins, CO). We are grateful for the advice and assistance of M. Boes, B. Cho, L. Filip, S. Lakdawala, A. Lee, K. Molvar, S. T. Palmacci, G. Paradis, L. Parameswaran, T. Schmidt, C. Wang, and C. Whitehurst. We greatly appreciate the assistance and support of E. Henchal, A. Mateczun, L. Peruski, and J. Gebhardt. This work was sponsored by A. Rudolph of the Defense Advanced Research Projects Agency's Defense Sciences Office and by A. Senecal of the U.S. Army Soldier and Biological Chemical Command's Combat Feeding Program under Air Force contract number F19628-00-C-0002. Opinions, interpretations, conclusions, and recommendations are those of the authors and are not necessarily endorsed by the Department of Defense.

Supporting Online Material

www.sciencemag.org/cgi/content/full/301/5630/213/DC1
Materials and Methods
Figs. S1 to S4
References

25 March 2003; accepted 5 June 2003

Suppression of Ovarian Follicle Activation in Mice by the Transcription Factor Foxo3a

Diego H. Castrillon,[1,2]* Lili Miao,[1] Ramya Kollipara,[1] James W. Horner,[1] Ronald A. DePinho[1]†

Foxo transcription factors have been implicated in diverse biological processes, including metabolism, cellular stress responses, and aging. Here, we show that *Foxo3a*$^{-/-}$ female mice exhibit a distinctive ovarian phenotype of global follicular activation leading to oocyte death, early depletion of functional ovarian follicles, and secondary infertility. Foxo3a thus functions at the earliest stages of follicular growth as a suppressor of follicular activation. In addition to providing a molecular entry point for studying the regulation of follicular growth, these results raise the possibility that accelerated follicular initiation plays a role in premature ovarian failure, a common cause of infertility and premature aging in women.

The FOXO subfamily of forkhead transcription factors consists of Foxo3a (FKHRL1), Foxo1 (FKHR), and Foxo4 (AFX), all downstream effectors of the PTEN/PI3K/AKT pathway (*1*). In *Caenorhabditis elegans*, systematic genetic analyses have revealed the existence of a conserved insulinlike signaling pathway involved in development, longevity, and fertility (*2–5*). Conservation of this pathway has fueled speculation that Foxo factors regulate related biological processes in mammals (*6*), prompting us to generate mice bearing a null mutation in the *Foxo3a* locus (fig. S1 and supporting online text). Despite a broad pattern of expression (fig. S1, D and E) (*7–9*), *Foxo3a*$^{-/-}$ animals were outwardly normal and did not show a prominent cancer-prone condition, abnormal weight gain (Fig. 1A), or statistically significant differences in mortality up to 48 weeks of age. *Foxo3a*$^{-/-}$ animals did exhibit some physiologic abnormalities, consistent with the view that Foxo3a serves diverse physiologic roles. Peripheral blood smears from *Foxo3a*$^{-/-}$ animals revealed hematologic abnormalities (apparent as early as 3 weeks of age), including a mild compensated anemia with associated reticulocytosis. *Foxo3a*$^{-/-}$ animals also exhibited a decreased rate of glucose uptake in glucose tolerance tests after an overnight fast (*10*).

Foxo3a$^{-/-}$ and control females bore first litters of similar sizes (supporting online text), indicating normal sexual maturation. However, in contrast to males, *Foxo3a*$^{-/-}$ females exhibited a marked age-dependent decline in reproductive fitness and were sterile by 15 weeks of age (Fig. 1B). Gross and histologic evaluation revealed no abnormalities of Müllerian structures or the pituitary in *Foxo3a*$^{-/-}$ females. Ovaries from *Foxo3a*$^{-/+}$ and *Foxo3a*$^{-/-}$ females showed no size differences through postnatal day (PD) 3. However, by PD8 to 14, ovaries from *Foxo3a*$^{-/-}$ mice were consistently enlarged (Fig. 2A).

In mammals, follicular growth is irreversible, and follicles recruited from the resting (primordial) follicle pool to the growing pool undergo apoptotic death (atresia) if not selected for further growth at subsequent stages of maturation (*11*). Follicular activation is characterized by oocyte growth and the transition of squamous to cuboidal granulosa cells (GCs), followed by GC proliferation (*12*). The activation of individual follicles involves unknown triggering mechanisms intrinsic to the ovary (*11*), although circulating factors likely modulate the overall rate of initiation (*13*). Follicular activation is independent of pituitary gonadotropins (*14*).

PD3 *Foxo3a*$^{-/+}$ and *Foxo3a*$^{-/-}$ ovaries had similar numbers of oocytes (Fig. 3A) and patterns of apoptosis (*10*). By PD14, however, *Foxo3a*$^{-/-}$ ovaries contained markedly elevated numbers of early-growing follicles characterized by an increased oocyte diameter and flattened GCs; mitotic activity began in more advanced primary follicles with cuboidal GCs (Fig. 2B). This pervasive activation of follicular growth in *Foxo3a*$^{-/-}$ females resulted in the progression of increased numbers of follicles to more advanced stages of follicular development. Compared with controls, PD14 *Foxo3a*$^{-/-}$ ovaries showed 1.9- and 2.1-fold increases in the number of primary and secondary follicles (Fig. 3C, $P = 0.012$ and 0.000) and in the number of atretic secondary follicles (Fig. 3C, $P = 0.016$). At 4.5 weeks of age, around the onset of sexual maturity, *Foxo3a*$^{-/-}$ ovaries still contained large num-

[1]Department of Medical Oncology, Dana-Farber Cancer Institute, and Departments of Medicine and Genetics, Harvard Medical School, Boston, MA 02115, USA. [2]Women's and Perinatal Pathology Division, Department of Pathology, Brigham and Women's Hospital, Harvard Medical School, Boston, MA 02115, USA.

*Present address: Laboratory of Molecular Pathology, Department of Pathology, University of Texas Southwestern Medical School, Dallas, TX 75390, USA.
†To whom correspondence should be addressed: E-mail: ron_depinho@dfci.harvard.edu